



POAC11-084

## **A MODIFIED DISCRETE ELEMENT MODEL FOR SEA ICE DYNAMICS**

Shunying Ji<sup>1</sup>, Anliang Wang<sup>1</sup>, Baohui Li<sup>2</sup>, Yu Liu<sup>2</sup>, Hai Li<sup>2</sup>

<sup>1</sup>Department of Engineering Mechanics, Dalian University of Technology, Dalian, China

<sup>2</sup>National Marine Environment Forecast Centre, Beijing, China

### **ABSTRACT**

Considering the non-continuous characteristics of sea ice at various scales, a modified discrete element model (DEM) was developed for sea ice dynamics based on granular material rheology. In this modified DEM, a soft sea ice particle is introduced with the ability of self-adjusting the particle size. Each ice particle is treated as an assembly of ice floes, and its concentration and thickness is adapted with the size change of ice particle under the mass conservation. The contact force among ice particles is calculated using a viscous-elastic model, while the maximum shear force is governed by the Mohr-Coulomb friction law. With this modified DEM, the ice flow dynamics in a channel are simulated with various widths under the drag of wind and current, the concentrations and velocities of ice particles are obtained, and reasonable dynamic process is analyzed. Moreover, the sea ice dynamic process in a vortex wind field is simulated to compare with the simulated results from particle-in-cell (PIC) method. With the consideration of the influence of thermodynamics, this modified DEM will be improved in the next study.

### **INTRODUCTION**

From field observations and satellite images, the sea ice behaves as a granular material obviously, and the level ice, ice ridge, rafted ice and open water appear together (Tremblay et al., 1997; Overland et al., 1998; Schulson, 2004). The ice floes have a large size range, which can be more than 100km on large scale, or less than 1m on small scale (Overland et al., 1998; Dempsey, 2000; Hibler, 2001). This discrete distribution of sea ice has been noticed in the early 1980's, and it was pointed out that the ice cover performs as a granular material (Rothrock, et al., 1984). The granular theory with regular disks was adopted firstly to simulate the ice floe collision in the broken ice fields (Shen et al., 1986; Lepparanta et al., 1990). Recently, the ice particle shape has been modified with irregular shape, and applied into the forming of ice ridge on meso-scale and sea ice evolution in arctic on large scale (Hoyland, 2002; Hopkins, 2004, 2006).

In the DEM of sea ice dynamics, the ice field is discretized into a series of discrete element under Lagrangian coordinates. Each ice element has its own thickness, velocity and size. Considering the frozen of ice floes, the ice breakup, rafting and ridging can also be simulated. The DEM has potentially great accuracy, since it has precise fixed and free edges to handle the complex boundary conditions. It can examine both aggregate and local behavior in the ice field. In addition, the DEM resembles the physical nature of sea ice dynamics. Therefore, the DEM of sea ice dynamics has the advantages of strong physical significance, and high computational precision.

In the conventional DEM, the ice cover is described as rigid blocks with constant size and

thickness. The huge computational cost of DEM is the key limitation. Therefore, a modified DEM is introduced here for sea ice dynamics. In this modified DEM, sea ice is modeled as an assembly of circular ice floes. Contacts are non-instantaneous and multiple contacts can occur simultaneously for each particle. Contact forces are modeled as viscous-elastic forces with a friction limit for the tangential component. Ridging effects are modeled by allowing particle size to change when contact stress exceeds a plastic yielding strength.

The particle plastic deformation is novel in this study, which can model the ice rafting and ridging with dynamic particle size, thickness and concentration. To verify this modified DEM, two numerical cases of sea ice dynamics are carried out. One is the ice flow process in a channel with various widths, and the other is the ice dynamics in a vortex wind field. Finally, the improvements and applications of this model are discussed.

## MODIFIED DISCRETE ELEMENT MODEL FOR SEA ICE DYNAMICS

### *Momentum equation*

The momentum equation for the motion of the ice element is governed by ice interactions, wind and water forces, Coriolis force, and ocean tilt effect. For each ice element, the momentum equation can be written as

$$M \frac{d\mathbf{V}}{dt} = -Mf\mathbf{K} \times \mathbf{V} + \boldsymbol{\tau}_a + \boldsymbol{\tau}_w - Mg\nabla \xi_w + \mathbf{F}_c \quad (1)$$

where  $M$  is the ice mass per unite area and  $M = N\rho_i h_i$  with  $\rho_i$  is the ice density,  $h_i$  is the ice thickness,  $N$  is the ice concentration;  $\mathbf{V}$  is the ice velocity vector,  $f$  is the Coriolis parameter,  $\mathbf{K}$  is a unit vector normal to the ice surface;  $\boldsymbol{\tau}_a$  and  $\boldsymbol{\tau}_w$  are the air and water stresses, here we have  $\boldsymbol{\tau}_a = \rho_a C_a |\mathbf{V}_{ai}| \mathbf{V}_{ai}$ ,  $\boldsymbol{\tau}_w = \rho_w C_w |\mathbf{V}_{wi}| \mathbf{V}_{wi}$ .  $\rho_a$  and  $\rho_w$  are the density of air and current, respectively.  $C_a$  and  $C_w$  are the drag coefficient of wind and current, respectively.  $\mathbf{V}_{ai}$  and  $\mathbf{V}_{wi}$  are the wind and current velocity vector relative to the ice, respectively.  $g$  is the gravity,  $\xi_w$  is the ice surface height, and  $\mathbf{F}_c$  is the force vector of one ice particle contacting with its neighbors. The key to solve the momentum equation is to determine the contact force vector  $\mathbf{F}_c$ .

### *Contact force model of sea ice particles*

The discrete element model for granular material simulations was established in the late 1970s, and has been improved perfectly recently. Here, we used a viscous-elastic model with Mohr-Coulomb friction law to simulate the interaction among ice particles.

The interaction among ice particles is determined with the elastic-viscous-plastic contact model. The contact force model mainly consists of three portions: normal and tangential damping force proportional to velocity, normal and tangential elastic force based on stiffness and overlap, shear sliding force based on Mohr-Coulomb friction law. The contact force model is shown in Fig. 1, where  $M_A$  and  $M_B$  are the mass of ice particle A and B,  $K_n$  and  $K_s$  are the normal and tangential stiffness,  $C_n$  and  $C_s$  are the normal and tangential damping coefficient, respectively,  $\mu$  is the friction coefficient. Using the contact force model above, the normal and tangential force of the two particles at contact can be calculated.

The normal force  $F_n$  consists of an elastic component  $F_e$  and a viscous component  $F_v$ , and can be determined with

$$F_n = F_e + F_v \quad (2)$$

Here, the elastic and viscous force can be written as

$$F_e = K_n x_n, \quad F_v = -C_n v_n \quad (3)$$

where  $x_n$  and  $v_n$  are the normal displacement and normal velocity of the two ice particles at contact.

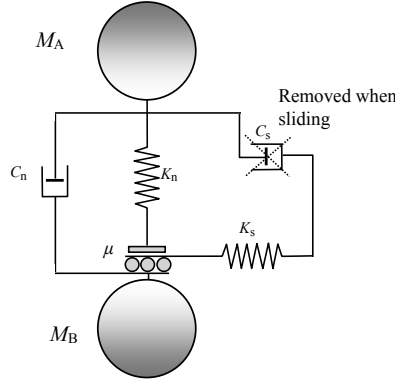


Figure 1. Contact force model for granular collision

Considering the influence of ice concentration, the normal stiffness coefficient  $K_n$  can be written as a function of concentration as

$$K_n = Eh_i \left( \frac{N_i}{N_{\max}} \right)^j \quad (4)$$

where  $E$  is the elastic modulus,  $N_{\max}$  is the maximum ice concentration, and  $j$  is an empirical constant. Normally, we have  $j = 15$  (Shen et al., 1990).

The normal damping coefficient can be calculated as

$$C_n = \zeta_n \sqrt{2MK_n}, \quad \zeta_n = \frac{-\ln e}{\sqrt{\pi^2 + \ln^2 e}} \quad (5)$$

where  $\zeta_n$  is the dimensionless normal damping coefficient,  $e$  is the restitution coefficient,  $M$  is the mean mass of two particles.

A slip condition is implemented for the tangential component. The tangential force is modeled by the spring-dashpot system until it reaches the friction limit, then the tangential force is modeled by the friction law. The friction limit is defined as

$$F_t = \min(K_s x_s - C_s v_s, \mu F_n) \quad (6)$$

where  $v_s$  is the shear component of particle velocity and  $\mu$  is the coefficient of friction.

#### **Normal contact force with plastic deformation**

This modified DEM adopts the concept of smoothed particle of hydrodynamics (SPH) approach, and one ice particle is an assembly of small ice floes. Therefore, the ice particle is not a real ice block, and has its statistical information depending on ice floes inside.

In this modified DEM, the novel portion is the plastic deformation, which considers the ice rafting and ridging. Since one particle in the DEM is constructed as an assembly of ice floes, the

particle size can be adjusted based on its interactions with neighbors, while its concentration and mean thickness can also be changed accordingly (as shown in Fig. 2). The sea ice floes have an initial dense packing in a sea ice package with high concentration (as shown in Fig. 2(a)). Under the action of wind and current, the ice cover can be packed in loose or dense conditions (as shown in Fig. 2(b)-(c)). In the dynamic process of ice particle size, the total mass of the ice particle is constant. When the concentration approaches its maximum value  $N_{max}$ , the mean thickness will increase with the decreasing of particle size (as shown in Fig. 2(d)).

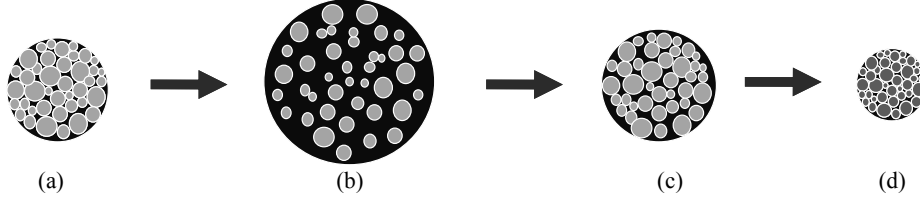


Figure 2. Dynamic evolution process of sea ice particle in the modified DEM

The determination of ice particle size, thickness and concentration are based on the calculation of normal stress and plastic deformation. A Mohr-Coulomb yielding limit is imposed on the particles to represent ice rafting and ridging. The Mohr-Coulomb yield surface is shown in Fig. 3. In the figure,  $c$  is the cohesion;  $\varphi$  is the ice friction angle;  $\sigma_1$  and  $\sigma_2$  are the principle stresses. This yielding function is determined by three parameters, namely frictional angle, cohesion and hydrostatic pressure. The friction angle  $\varphi$  may vary with ice conditions. Shen et al. (1990) and Coon (1998) adopted  $46^\circ$  and  $52^\circ$  in river and sea ice simulations. In this paper, we use  $c=0$  and  $\varphi=46^\circ$ .

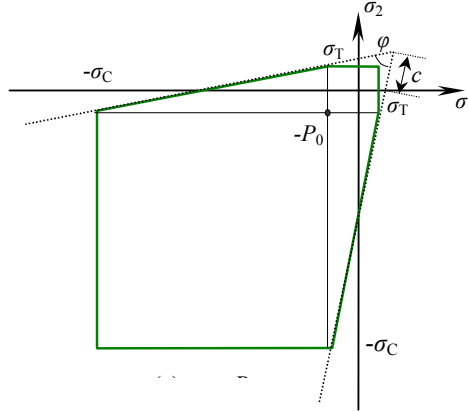


Figure 3. Mohr-Coulomb yielding criterion in 3D

The Mohr-Coulomb yield curve is constructed with three couple lines, i.e. shear, compressive and tensile surfaces, and can be written as

$$\sigma_1 = K_D \sigma_2 + 2c\sqrt{K_D} \quad (7)$$

$$\sigma_C = -K_C P_0 - 2c\sqrt{K_C} \quad (8)$$

$$\sigma_T = -K_D P_0 + 2c\sqrt{K_D} \quad (9)$$

here  $K_D = \tan^2(\pi/4 - \varphi/2)$  and  $K_C = \tan^2(\pi/4 + \varphi/2)$ . In the vertical direction, the normal stress

$\sigma_{zz}$  is a function of ice depth (Ji et al., 2005). Considering the influence of ice concentration, the mean vertical hydrostatic pressure can be written as (Shen et al. 1990; Ji et al., 2005)

$$P_0 = \left(1 - \frac{\rho_i}{\rho_w}\right) \frac{\rho_i g t_i}{2} \left(\frac{N}{N_{\max}}\right)^j \quad (10)$$

where  $P_0$  is the mean pressure in the vertical direction. The horizontal hydrostatic pressure can be calculated as

$$P_r = K_0 P_0 \quad (11)$$

where  $P_r$  is the horizontal hydrostatic pressure;  $K_0$  is the transfer coefficient, which can be determined with experiments. In broken ice field without cohesion, we have  $K_0 = 1 - \sin \varphi$ .

Plastic deformation is modelled by changing the particle diameter, concentration, and thickness, while particle mass is constant. Thickness only changes when concentration reaches a maximum limit. When ridging effects are included, the normal elastic force is limited by a plastic stress limit  $\sigma_p$ , which is the internal ice pressure term introduced by Shen et al. (1990):

$$\sigma_p = \tan^2\left(\frac{\pi}{4} + \frac{\varphi}{2}\right) \left(1 - \frac{\rho_i}{\rho_w}\right) \frac{\rho_i g h_i}{2} \left(\frac{N_i}{N_{\max}}\right)^j \quad (12)$$

where  $\varphi$  is the ice internal friction angle. If normal stress exceeds  $\sigma_p$ , normal stress is set to  $\sigma_p$  and plastic deformation occurs. In this way the model includes ridging effects. Plastic deformation is defined as the difference between total and elastic deformation, where total deformation is the compression distance  $x_n$ , and elastic deformation is due to the maximum elastic stress,  $\sigma_p$ . A Mohr-Coulomb yielding limit is imposed on the particles to represent ice ridging. Any stress exceeding the yielding criterion, results in particle deformation.

## NUMERICAL SIMULATION OF SEA ICE DYNAMICS WITH MODIFIED DEM

### *Sea ice flow in a channel with various widths*

A channel with various widths is covered partly by a uniform layer of ice with initial ice thickness  $t_{i0}$  and concentration  $N_0$ . The layout of the channel is shown in Fig. 4. At the mouth of the left bell mouth, an ice boom is built. Under constant wind and current drag, the sea ice flows downstream, while the ice concentration and thickness changes with the particle size. After some time of ice ridging, the ice boom is removed, and the ice flows through the narrow portion of the channel, and rafts and ridges at the end of the channel. The ice flow process in this channel with various widths is simulated with the modified DEM. The input parameters are listed in Table 1.

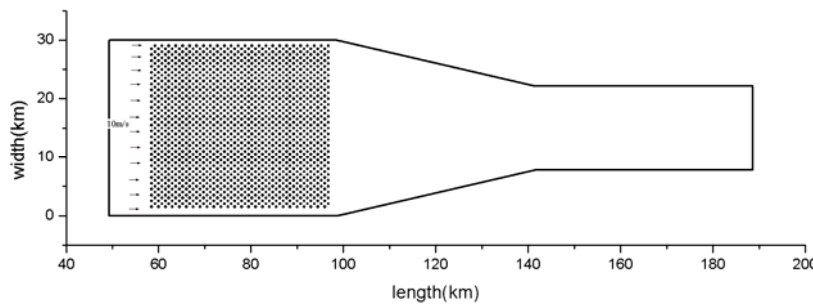


Figure 4. Width-averaged ice thickness simulated and analytical solution

Table 1. Parameters used in the ice ridging simulation

Parameter	Definition	Value	Parameter	Definition	Value
$B$	Width of ice field (m)	500	$L$	Initial ice length (m)	4500
$t_{i0}$	Initial ice thickness (m)	0.2	$N_0$	Initial ice concentration (%)	80
$C_a$	Wind drag coefficient	0.015	$C_w$	Current drag coefficient	0.0045
$V_a$	Wind speed (m/s)	10.0	$V_w$	Current speed (m/s)	0.2
$\rho_i$	Ice density (kg/m <sup>3</sup> )	917	$\rho_w$	Water density (kg/m <sup>3</sup> )	1017
$\mu$	Friction coefficient	0.5	$\varphi$	Friction angle of ice floe (°)	46
$E$	Young's Modulus (MPa)	10	$\Delta t$	Time step (s)	1.83

With the modified DEM, the velocity and concentration of ice flow in the channel are plotted in Fig. 6. Under the given wind and current drag, the sea ice is jammed in front of the middle ice boom after 6 days. We can find the ice concentration approaches the maximum value  $N_{\max} = 1.0$  around the ice boom, then decreases with increasing distance to the boom. Under the action of the inclined bank, the ice particle moves into the channel centre. With the removal of ice boom after 8 days, the ice flow releases and flows to the end of the channel. While the ice concentration decreases under the action of ice pressure. After 12 days, the sea ice jams at the downstream boom and approaches steady state again. With this modified DEM, the ice flow process is simulated well, and the distribution of ice velocity, concentration and thickness can be obtained at various times.

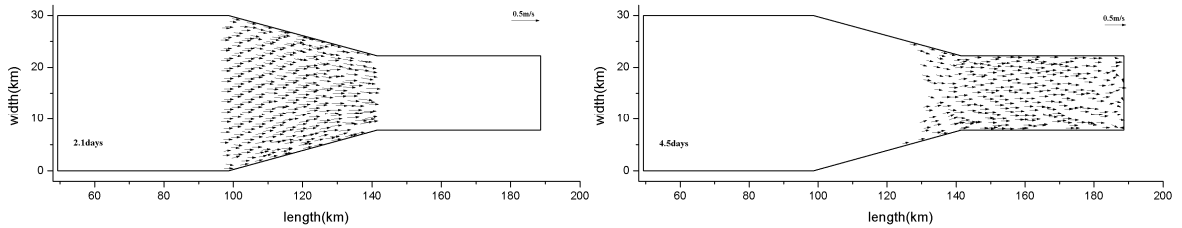
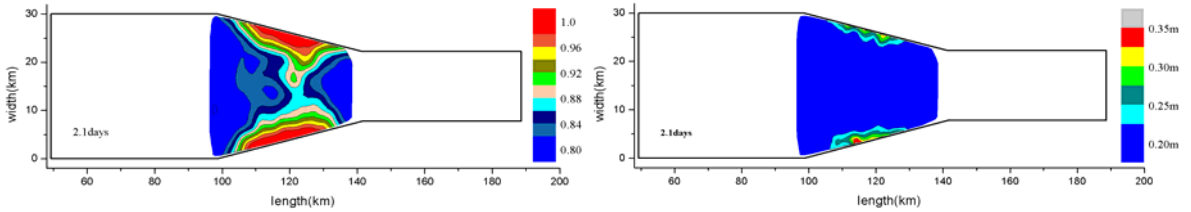


Figure 5. Ice thickness and velocity distributions simulated with the modified DEM



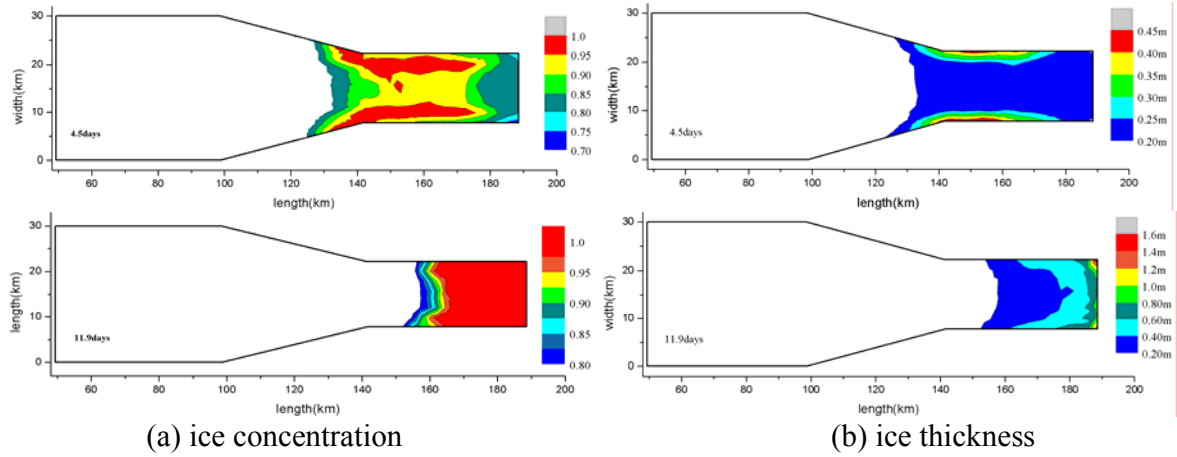


Figure 6. Ice concentration and thickness contours simulated with the modified DEM

### *Sea ice dynamics in a vortex wind field*

As a classical numerical case for sea ice dynamics, the ice drifting in a vortex wind field was constructed by Flato(1993) first to estimate the PIC approach. Here, this vortex wind field is also adopted to verify the modified DEM simulation. In this vortex wind field test, the upper half of  $500\text{km} \times 500\text{km}$  rectangular domain is covered by uniform ice cover with thickness of 0.2m and concentration of 0.80, shown as Fig.7. The lower half is open water, and the vortex centre position is (250km, 200 km).

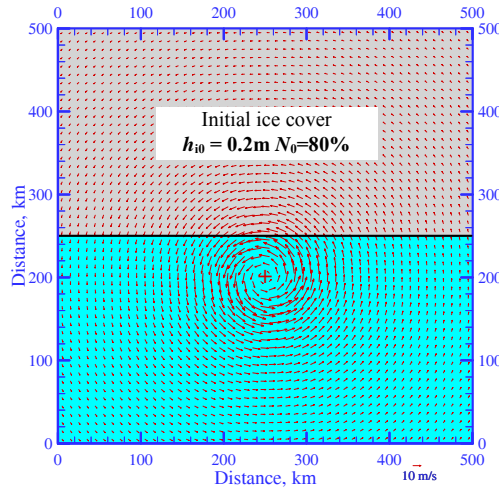


Figure 7. Vortex wind field and initial sea ice distribution

The sea ice dynamical process in the vortex wind field is simulated for 8 days with the modified DEM. The time step is 6s, particle size is 5km. The simulated ice particle velocity and concentration from the first to fifth day are plotted in Fig. 8. It can be found that the ice flows around the vortex centre under the action of vortex wind. In the evolution of ice flow, the ice velocity has the similar distribution with wind field. It is faster and closer to the wind centre. As for the ice concentration, we can find the ice has a divergent trend. The ice has a lower concentration around the vortex wind centre. The ice edge around the vortex centre has a sharp shape, which shows high precision of the developed model.

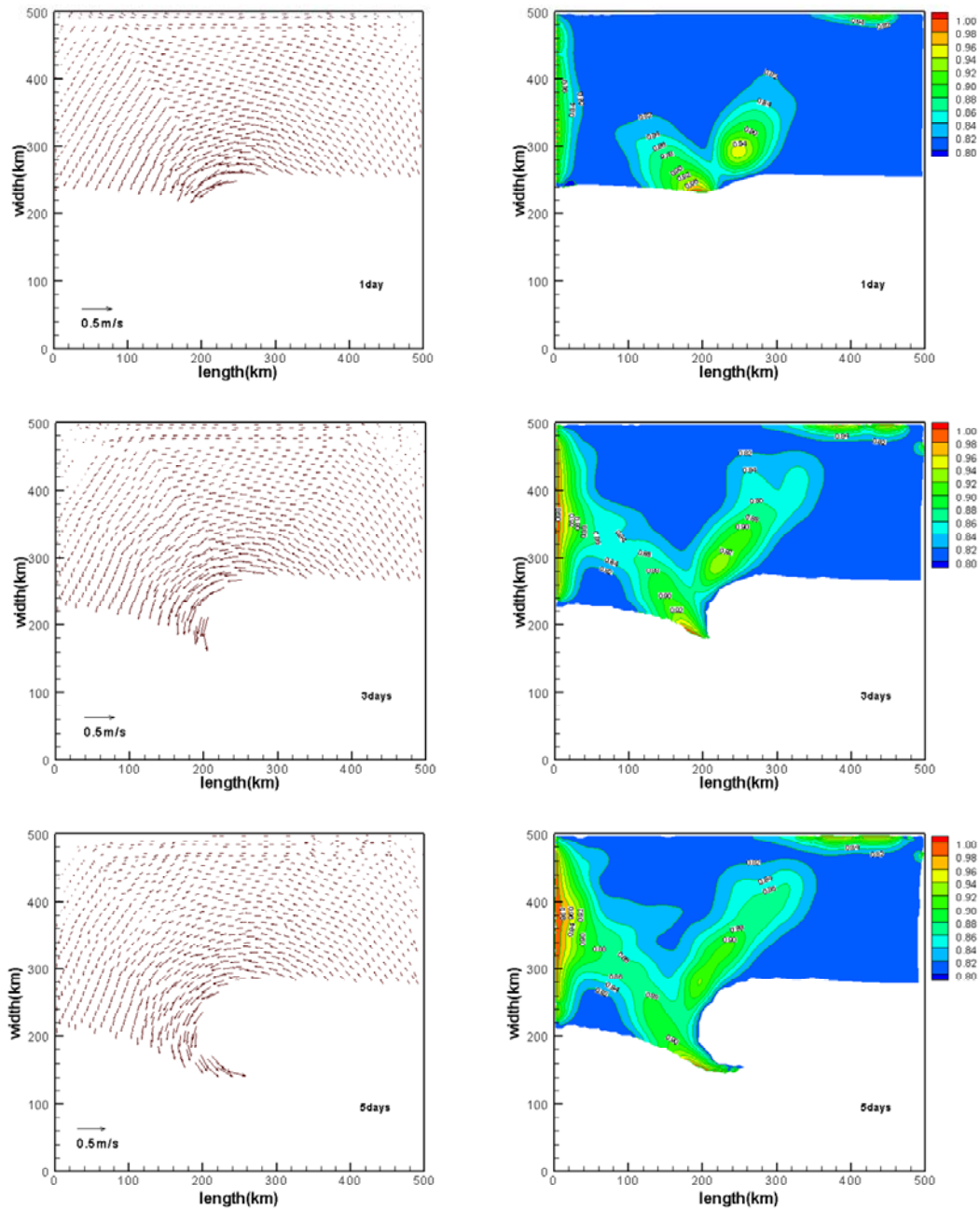


Figure 8. Velocity vector and concentration of sea ice simulated with Modified DEM

## CONCLUSIONS

The dynamics of ice cover perform as an uncontinuum material on large and small scale in polar and sub-polar oceans. To model the sea ice dynamics, a modified discrete element model was developed. In this model, the sea ice particle is treated as an assembly of ice floes with various concentration and thickness. The interaction of ice particle is calculated with a viscous-elastic-plastic contact force model. In the dynamic process of ice drifting, the size of ice particle can be adjusted under the action of the external and internal ice forces. The concentration and thickness can be determined accordingly based on the conservation of ice mass. The normal force between

ice particles is limited with the plastic yielding, which can cause the rafting and ridging of ice cover. With this modified DEM, two numerical cases of sea ice dynamics are carried out. One is the ice flow in a channel with various widths. The other is the ice drifting in a rectangular domain under a vortex wind field. Both of the two cases show the reasonable dynamic processes simulation with the modified DEM. In the future studies, the thermodynamics and refrozen of ice floes will be considered to improve the precision. With this improvement, the sea ice growth and drifting can be simulated with more reliability.

## REFERENCES

- Coon, M. D. and Knoke, G. S. and Pritchard, R., 1998. The architecture of an anisotropic elastic-plastic sea ice mechanics constitutive law. *Journal of Geophysical Research*, 103(C10): 21915 -21925.
- Dempsey, J. P., 2000. Research trends in ice mechanics. *International Journal of Solids and Structures*, 37: 131-153.
- Flato, G. M., 1993. A particle-in-cell sea-ice model. *Atmosphere and Oceanography*. 31(3): 339-358.
- Hibler, W. D., 2001. Sea ice fracturing on the large scale. *Engineering Fracture Mechanics*, 68: 2013-2043.
- Hopkins, M. A., Frankenstein, S. and Thorndike, A. S., 2004. Formation of an aggregate scale in arctic sea ice. *Journal of Geophysical Research*, 109(C01032):1-10.
- Hopkins, M. A. and Thorndike, A. S., 2006. Floe formation in arctic sea ice. *Journal of Geophysical Research*, 111, C11S23, doi:10.1029/2005JC003352.
- Hoyland. K. V., 2002. Simulation of the consolidation process in first-year sea ice ridges. *Cold Regions Science and Technology*, 34: 143-158.
- Lepparanta, M., Lensu, M. and Lu, Q. M., 1990. Shear flow of sea ice in the Marginal Ice Zone with collision rheology. *Geophysica*, 25(1-2):57-74.
- Ji, S., Shen, H. T., Wang Z., et al., 2005. A viscoelastic-plastic constitutive model with Mohr-Coulomb yielding criterion for sea ice dynamics. *Acta Oceanologica Sinica*, 24(4): 54-65.
- Overland, J. E., McNutt, S. L. and Salo S., 1998. Arctic sea ice as a granular plastic. *Journal of Geophysical Research*, 103(C10): 21845-21868.
- Rothrock, D. and Thomdike, A. S., 1984. Measuring the sea ice grain size distribution. *Journal of Geophysical Research*, 89(C4):6477-6486.
- Schulson, E. M., 2004. Compressive shear faults within arctic sea ice: Fracture on scales large and small. *Journal of Geophysical Research*, 109(C07016):1-23.
- Shen, H. H. and Hibler, W. D., 1986. Lepparanta M. On applying granular flow theory to a deforming broken ice field. *Acta Mechanica*, 63: 143-160.
- Shen, H. T., Shen, H. H. and Tsai, S. M., 1990. Dynamic transport of river ice. *Journal of Hydraulic Research*, 28(6):659-671.
- Tremblay, L. B. and Mysak, L. A., 1997. Modeling sea ice as a granular material, including the dilatancy effect. *Journal of Physical Oceanography*, 27:2342-2360.